Oncogene (2015) **34,** 3240–3250

www.nature.com/onc

ORIGINAL ARTICLE

miR-340 inhibits tumor cell proliferation and induces apoptosis by targeting multiple negative regulators of p27 in non-small cell lung cancer

S Fernandez[1], M Risolino[1], N Mandia[1], F Talotta[1], Y Soini[2], M Incoronato[3], G Condorelli[4], S Banfi[5] and P Verde[1,3]

MicroRNAs (miRNAs) control cell cycle progression by targeting the transcripts encoding for cyclins, CDKs and CDK inhibitors, such as $p27^{KIP1}$ (p27). p27 expression is controlled by multiple transcriptional and posttranscriptional mechanisms, including translational inhibition by miR-221/222 and posttranslational regulation by the SCF^{SKP2} complex. The oncosuppressor activity of miR-340 has been recently characterized in breast, colorectal and osteosarcoma tumor cells. However, the mechanisms underlying miR-340-induced cell growth arrest have not been elucidated. Here, we describe miR-340 as a novel tumor suppressor in non-small cell lung cancer (NSCLC). Starting from the observation that the growth-inhibitory and proapoptotic effects of miR-340 correlate with the accumulation of p27 in lung adenocarcinoma and glioblastoma cells, we have analyzed the functional relationship between miR-340 and p27 expression. miR-340 targets three key negative regulators of p27. The miR-340-mediated inhibition of both *Pumilio* family RNA-binding proteins (PUM1 and PUM2), required for the miR-221/222 interaction with the *p27* 3′-UTR, antagonizes the miRNA-dependent downregulation of p27. At the same time, miR-340 induces the stabilization of p27 by targeting SKP2, the key posttranslational regulator of p27. Therefore, miR-340 controls p27 at both translational and posttranslational levels. Accordingly, the inhibition of either PUM1 or SKP2 partially recapitulates the miR-340 effect on cell proliferation and apoptosis. In addition to the effect on tumor cell proliferation, miR-340 also inhibits intercellular adhesion and motility in lung cancer cells. These changes correlate with the miR-340-mediated inhibition of previously validated (*MET* and *ROCK1*) and potentially novel (*RHOA* and *CDH1*) miR-340 target transcripts. Finally, we show that in a small cohort of NSCLC patients ($n = 23$), representative of all four stages of lung cancer, miR-340 expression inversely correlates with clinical staging, thus suggesting that miR-340 downregulation contributes to the disease progression.

Oncogene (2015) **34,** 3240–3250; doi:10.1038/onc.2014.267; published online 25 August 2014

INTRODUCTION

MicroRNAs (miRNAs) have a strong impact on all the main aspects of tumorigenesis by controlling the major regulators of cell cycle progression, senescence, apoptosis and autophagy, along with tumor cell motility, invasion and metastasis.[1–3] miRNA-mediated posttranscriptional regulation requires the activity of multiple RNA-binding proteins, which contribute to the functions of miRNAs in tumorigenesis.[4]

Altered expression of miRNAs targeting cyclins, CDKs or CDK inhibitors, is involved in deregulation of cell cycle progression during tumorigenesis. Among oncosuppressor miRNAs, the miR--15/16 family members inhibit cell cycle progression by targeting CCND1/2/3, CCNE1 and CDK4, while the p53-regulated miR-34 family inhibits the expression of CCND1 and CCNE2, along with CDK4 and CDK6.[5–7] In contrast, overexpression of oncomiRs results in the downregulation of the main CDK inhibitors (CDKNs), such as the CDKN1 family members. For example, $p21^{CIP1}$ is down-regulated by two members (miR-106b and miR-93) of the oncogenic miR-106b-25 miRNA cluster,[8] while both p27 and p57 transcripts are targeted by the closely related miR-221 and miR-222 oncomiRs.[9,10]

p27 represents the key target of miR-221/222 in prostate adenocarcinoma and glioblastoma cells,[9–11] papillary thyroid carcinoma,[12] hepatocellular carcinoma[13] and triple-negative breast cancer.[14] In lung cancer, miR-221/222 overexpression is clinically relevant. Accordingly, the miR-221/222-mediated down-regulation of p27 contributes to resistance of non-small cell lung cancer (NSCLC) cells to TRAIL-induced apoptosis.[15] The miR-221--/222-mediated control of p27 requires the expression of a *Pumilio* family RNA-binding protein Pumilio-1 (PUM1). In response to growth factor stimulation, PUM1 is upregulated and phospho-rylated, leading to its binding to the *p27* 3′-UTR. The interaction with PUM1 causes a conformational switch, which renders the *p27* 3′-UTR accessible to miR-221/222.[16]

miRNA-mediated control is one of the posttranscriptional mechanisms responsible for p27 downregulation in cancer cells. p27 posttranslational regulation is mediated by multiple phos-phoacceptor sites, controlling both nucleo-cytoplasmic shuttling and stability of the protein. Following phosphorylation by cyclin E-CDK2 on Thr187, p27 is polyubiquitylated by SCF^{SKP2}, prior to proteasomal degradation.[17] The F-box family member SKP2 (S-phase Kinase associated Protein 2) is the substrate specificity

[1]CNR Institute of Genetics and Biophysics, Naples, Italy; [2]Institute of Clinical Medicine, Pathology and Forensic Medicine, School of Medicine, Cancer Center of Eastern Finland, University of Eastern Finland, Kuopio, Finland; [3]IRCCS SDN, Naples, Italy; [4]Department of Cellular and Molecular Biology and Pathology, "Federico II" University of Naples, Naples, Italy and [5]Telethon Institute of Genetics and Medicine (TIGEM), Naples, Italy. Correspondence: Dr P Verde, CNR Institute of Genetics and Biophysics, Via P. Castellino 111, Naples 80123, Italy.
E-mail: pasquale.verde@igb.cnr.it
Received 15 February 2014; revised 29 June 2014; accepted 14 July 2014; published online 25 August 2014

component of the SCF^{SKP2} (SKP1/Cullin/F-box protein:SKP2) E3 ubiquitin ligase complex. p27 is the main functional target of Skp2,[18] as shown by the *in vivo* deletion of *Cdkn1B*, encoding for p27, which is sufficient to rescue the phenotype of the $Skp2^{-/-}$ mouse.[19] SKP2 overexpression inversely correlates with p27 accumulation in a large variety of solid tumors, including prostate, breast, ovarian, lung and metastatic melanoma.[17] During cell cycle progression, SKP2 expression is induced by oncogenic transcription factors, whereas SKP2 posttranslational regulation, mediated by multiple phosphoacceptor residues, controls the stability, localization and activity of the protein.[17] Although multiple regulatory mechanisms are implicated in the oncogenic upregulation of SKP2, we are not aware of miRNA-mediated control of SKP2 during human tumorigenesis.

Pathogenic, diagnostic and prognostic roles of miRNAs have been extensively studied in lung cancer. miRNAs have emerged as important biomarkers for lung cancer risk stratification and outcome prediction (reviewed in Lin *et al.*[20]).

In addition, miRNAs represent promising tools against lung cancer, as shown by the tumor regression obtained by *in vivo* delivery of *let-7*- or miR-34- family members.[21] These findings point to the basic and translational relevance of studying oncosuppressor miRNAs in lung cancer.

Here, we describe the role of miR-340 as a novel oncosuppressor miRNA in NSCLC.

RESULTS

miR-340 overexpression inhibits cell cycle progression and induces apoptosis in A549 cells

In agreement with our recent report,[22] miR-340 overexpression strongly inhibited the proliferation of NSCLC A549 cells. *Vice versa*, an anti-miR-340 locked nucleic acid (LNA) inhibitor significantly increased A549 cell viability (Figure 1a).

Therefore, we analyzed the effects of miR-340 on cell cycle distribution. miR-340 caused a significant increase of the G0/G1 population (from 59 to 80%), associated with a decrease of both S-phase (from 21 to 7%) and G2/M (from 20 to 12%) cell fractions (Figure 1b). The miR-340-induced inhibition of DNA synthesis was further analyzed by investigating the BrdU incorporation: a 60% decrease of BrdU-positive cells was detected in response to miR-340 overexpression, whereas the miR-340 inhibitor caused a 29% increase (Figures 1c and d).

Because of the significant fraction of floating rounded cells and condensed nuclei in miR-340-overexpressing cells (Figure 1e), we analyzed the apoptotic cascade. Proteolytically cleaved PARP was significantly increased in miR-340- vs control-mimic-transfected cells, whereas the miR-340 inhibitor exerted the opposite effect (Figure 1f). Accordingly, the activity of effector caspases (3/7) exhibited a twofold increase in response to the ectopic miR-340, but was significantly decreased when A549 cells were treated with the miR-340 inhibitor (Figure 1g).

miR-340-induced growth inhibition correlates with the upregulation of p27 mediated by the CDKN1B 3′-UTR

To dissect the mechanisms of miR-340-induced cell growth inhibition, we analyzed the effect of miR-340 on various cell cycle regulators in A549 cells. Strong accumulation of p27 was detected in response to the miR-340 mimic, compared with the control scramble oligonucleotide, whereas the LNA inhibitor significantly inhibited the p27 expression (Figure 2a). The other major CDKN1 family member, $p21^{CIP1}$, was unaffected by miR-340 overexpression or inhibition (not shown).

To extend our analysis to another cell type, and because of reported evidence of miR-340 downregulation in glioblastoma,[23,24] we overexpressed miR-340 in T98G glioblastoma cells. p27 was strongly accumulated in response to miR-340, whereas the anti-miR-340 LNA inhibited p27 expression in T98G cells (Figure 2b).

As in A549 cells, miR-340 overexpression dramatically inhibited the T98G cell viability, whereas the LNA inhibitor increased the proliferation rate (Figure 2c). Therefore, on the basis of the results of Figure 2a, we postulated that miR-340 could affect the expression of negative posttranscriptional regulators of p27.

miR-340 inhibits the miR-221/222-mediated downregulation of p27 by targeting the RNA-binding proteins PUM1 and PUM2

One recently described p27 control mechanism is represented by the miR-221/222-mediated posttranscriptional inhibition (reviewed in le Sage *et al.*[25]). By analyzing the top-ranking transcripts in the lists of miR-340 targets generated by the CoMeTa[22] and TargetScan (Release 6.2) algorithms, we found that both *Pumilio* family RNA-binding proteins, *PUM1* and *PUM2* (Pumilio-2), despite the divergence between their 3′-UTRs, contain potential miR-340 target sites. Because both PUM1 and PUM2 are required for repression of p27 by miR-221 and miR-222,[16] which are expressed and functional in A549 cells,[26] we postulated that p27 upregulation could result from the miR-340-mediated downregulation of PUM1 (and/or PUM2) and consequent abrogation of p27 inhibition by miR-221/222.

Therefore, we analyzed the expression of PUM1 and PUM2 in response to miR-340. In agreement with bioinformatic predictions, both *Pumilio* family members were strongly downregulated in response to the miR-340 mimic, whereas the LNA inhibitor induced the accumulation of both PUM1 and PUM2 (Figure 3a). Surprisingly, the dramatic changes of protein levels were not accompanied by significant modifications of cognate transcripts (Supplementary Figure S1A). To validate both transcripts as direct targets of miR-340, we generated several reporter constructs containing the 3′-UTR fragments encompassing the two miR-340 target sites of *PUM1,* or the three miR-340 target sites of *PUM2* (Figures 3b and c). Transfection analysis showed that only the fragment containing the *PUM1* 3′-UTR downstream site significantly inhibited the reporter activity, whereas the control vector was unaffected by the co-expressed miR-340. One site-directed mutation within the seed-matching sequence in the *PUM1* 3′-UTR downstream site significantly decreased the miRNA-mediated repression (Figure 3b).

Similarly, we generated other constructs containing the upstream site or the two downstream sites of the *PUM2* 3′-UTR. The upstream region was not significantly affected by miR-340, whereas the downstream fragment mediated a twofold decrease of luciferase activity. Site-directed mutations hitting each of the two seed sequences caused partial loss of the miR-340-mediated inhibition only for the upstream site (Figure 3c). Remarkably, both sites affected by mutations in the *PUM1* and *PUM2* 3′-UTRs are evolutionally conserved (Supplementary Figure S1B,C). Therefore, both the *PUM1* and *PUM2* 3′-UTRs are targeted by miR-340 and at least two of the *in silico* predicted sites are implicated in the miRNA-mediated repression.

Then, we tested if downregulation of PUM1 or PUM2 could affect the p27 expression level. After knocking down either PUM1 or PUM2 expression, we observed significant accumulation of p27 in A549 cells. The knockdown of both PUM family members did not further increase the p27 expression level (Figure 3d). These results showed that each of the two *Pumilio* family members was independently able to recapitulate the effect of miR-340 on p27 expression.

To test whether miR-340 was able to interfere with the miR-221/222-mediated downregulation of p27, we analyzed the effect of miR-222 in the presence of miR-340 or a PUM1-specific siRNA. As expected, miR-222 overexpression caused p27 downregulation (Figure 3e; compare lane 1 with lane 5),

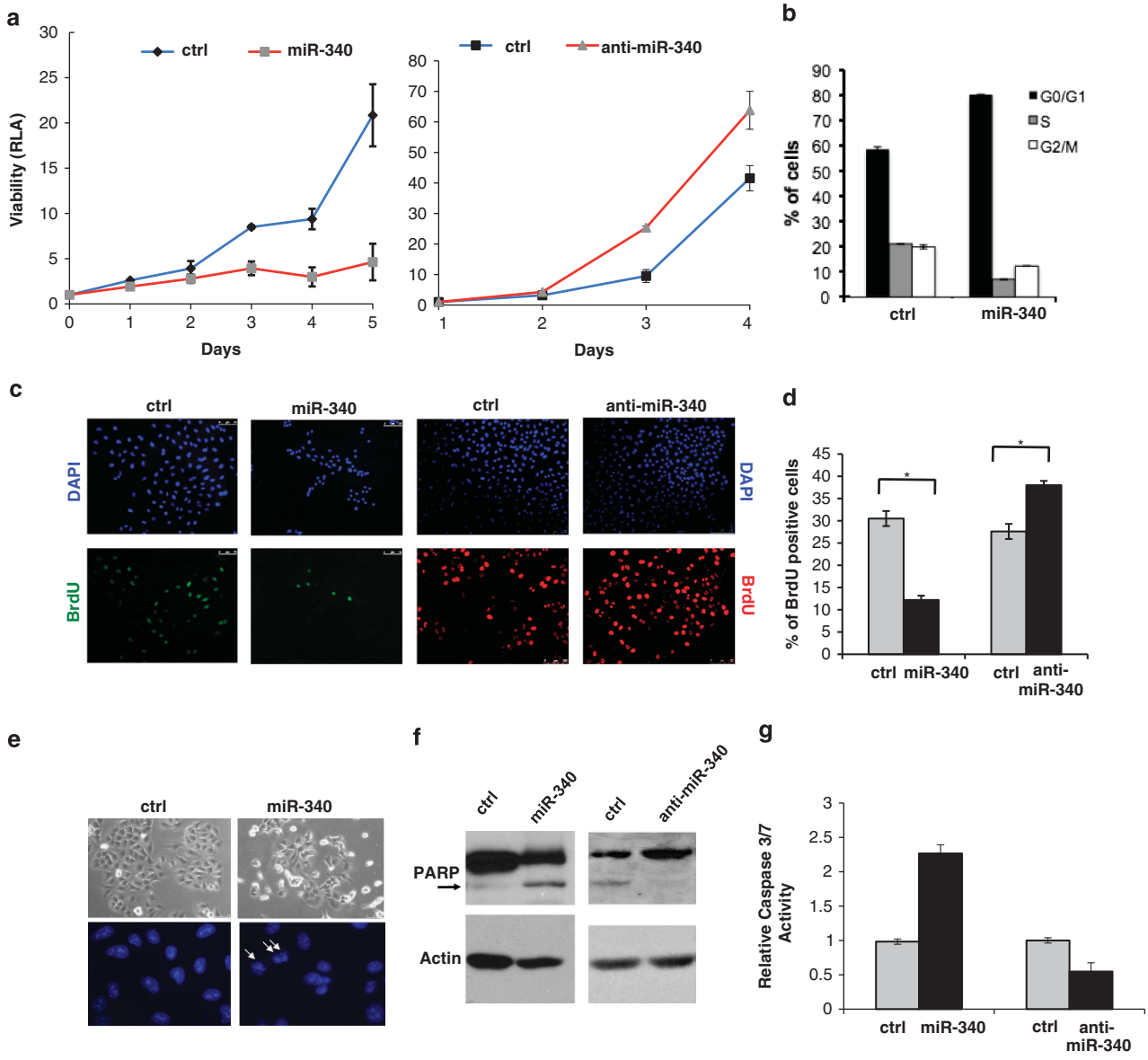

Figure 1. miR-340 overexpression induces growth arrest and apoptosis in A549 cells. (**a**) Growth rate of A549 cells transfected with miR-340 mimic or LNA anti-miR-340 vs mimic or LNA control. Viable cells were determined by luminometric assays at the indicated time points (**b**) FACS analysis of propidium iodide-stained A549 cells transfected with miR-340 mimic vs mimic control after 48 h. (**c**) Immunofluorescence analysis of BrdU incorporation in A549 cells transfected with miR-340 mimic or LNA anti-miR-340 vs mimic or LNA control for 72 h. BrdU was stained with FITC or Texas Red-conjugated antibodies in mimic- or LNA-transfected cells, respectively. Cell nuclei were visualized by DAPI staining. (**d**) Quantitation of BrdU staining results. Five different fields were analyzed. Error bars represent the mean ± s.d. of three independent experiments. Two-tail *t*-test results are indicated by $*P \leqslant 0.05$. (**e**) Morphology of A549 cells, 72 h after transfection with miR-340 mimic vs control. Right (DAPI staining): the arrows indicate representative condensed nuclei. (**f**) Western blotting analysis of full length (FL) and cleaved (C) PARP 72 h after transfection with miR-340 mimic or LNA inhibitor vs controls. Beta-actin serves as a loading control. (**g**) Luminometric assay of caspase 3/7 activity in A549 cells transfected with miR-340 mimic or LNA anti-miR-340 vs mimic or LNA controls 72 h after transfection. Error bars represent the mean ± s.d. of three independent experiments. Two-tail *t*-test results are indicated by $*P \leqslant 0.05$.

which was abrogated when miR-222 was expressed along with miR-340 or the PUM1-specific siRNA (lanes 6 and 8). Similarly, we found that silencing PUM2 partially inhibited the miR-222-mediated inhibition of p27 (Supplementary Figure S2A). We also ruled out that the observed effects could result from the miR-340-mediated inhibition of miR-221/222, because we observed that both miRNAs were only slightly upregulated, in response to miR-340 overexpression or downregulation (Supplementary Figure S2B).

The data in Figures 3d and e and Supplementary Figure S2 indicated that miR-340 was able to antagonize the miR-222-dependent downregulation of p27 by a PUM1/2-dependent mechanism. To show that the miR-340 effect was actually mediated by the miR-221/222 target site, we analyzed the expression of a luciferase reporter construct containing the 3′-UTR of the *p27* mRNA. Luciferase activity exhibited an almost-twofold increase in response to miR-340 and the siRNA-mediated inhibition of PUM1 exerted a similar effect (Figure 3f). Accordingly, miR-340 similarly stimulated the activity of the same reporter in the T98G cell line (Figure 3g), thus showing that the miR-340 effect on p27 accumulation was mediated, at least in part, by a mechanism impinging on the *p27* 3′-UTR.

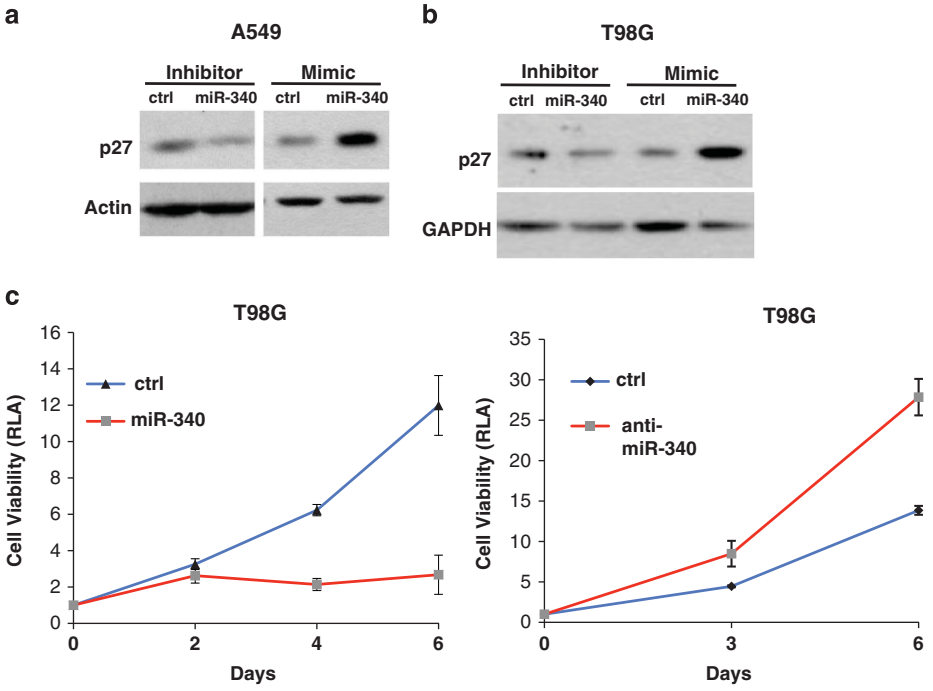

Figure 2. Induction of p27 expression by miR-340. (**a**) Western blotting analysis of p27 levels in A549 cells transfected for 48 h with LNA anti-miR-340 or miR-340 mimic vs LNA or mimic controls. The beta-actin signals, for control of equal loading, are the same as in Figures 3a and 5b, because the samples derive from the same blot. (**b**) Western blotting analysis of p27 levels in T98G cells transfected for 48 h with LNA anti-miR-340 or miR-340 mimic vs LNA or mimic controls (by densitometric analysis and normalization vs the GAPDH signal, p27 exhibited a 25% decrease, following treatment with the miR-340 inhibitor). (**c**) Growth rate of T98G cells transfected with miR-340 mimic or LNA anti-miR-340 vs mimic or LNA controls. Viable cells were determined by luminometric assays at the indicated time points. Error bars represent the mean ± s.d. of three independent experiments.

miR-340 induces the stabilization of p27 by targeting the transcript encoding for SKP2 ubiquitin ligase

The p27 accumulation after knocking down PUM1/2 was relatively smaller than the p27 induction in response to miR-340 (compare Figures 3d and 2a). Therefore, we investigated other aspects of p27 regulation.

Because ubiquitylation-dependent proteasomal degradation is the major mechanism controlling p27 during the cell cycle, we analyzed the p27 turnover in response to miR-340. The significantly increased p27 half-life (from about 2 h to over 8 h) in cells overexpressing miR-340 (Figures 4a and b) prompted us to postulate that miR-340 could impair p27 ubiquitylation. The SCF^{SKP2} (Skp/Cul/F-box) ubiquitin ligase complex is the main regulator of p27 turnover. The substrate-recognizing subunit, SKP2, is encoded by three alternatively spliced transcripts. While the first and third variant (a 3520-nt mRNA expressing a 424-aa protein and a 3273-nt mRNA expressing a 210 aa protein) share the same (2288-nt long) 3′-UTR, the second variant (1498-nt encoding for the 410-aa SKP2 isoform) contains a very short 3′-UTR (34-nt), including one bioinformatically predicted miR-340 site (Supplementary Figure S3A). All three mRNA isoforms were expressed in A549 cells (Supplementary Figure S3B). miRNA target prediction databases (TargetScan v.6.2, miRanda, PicTar), which include two short (143 and 34-nt) *SKP2* 3′-UTR isoforms, do not allow the analysis of the entire long *SKP2* 3′-UTR. However, through the analysis of the full-length *SKP2* 3′-UTR by using RNAHybrid,[27] we could identify four miR-340 target sites in the full size 2288-nt human *SKP2* 3′-UTR (Supplementary Figure S3C).

Then, we tested if *SKP2* expression was affected by miR-340 overexpression or functional inhibition. By using primers detecting all three isoforms, the *SKP2* mRNA was strongly downregulated in response to miR-340 overexpression and increased in response to the LNA inhibitor (Figure 5a). Immunoblotting showed that SKP2 expression was almost completely suppressed in response to the miRNA overexpression, and significantly upregulated in response to the anti-miR-340 (Figure 5b). We then investigated if SKP2 downregulation could recapitulate the miR-340 effect on p27 expression. As expected, the siRNA-mediated inhibition of SKP2 resulted in a strong concentration-dependent increase of p27 in A549 cells (Figure 5c). Then, we extended the analysis of the miR-340-mediated changes of PUM1, PUM2 and SKP2 to another cell system (HEK293), expressing high levels of miR-340 (Supplementary Figure S7). Along with the LNA inhibitor, we utilized a miRNA sponge expression vector, containing seven bulged binding sites for miR-340.[28] The three proteins were upregulated in response to both the LNA and the sponge inhibitor, thus suggesting that their respective transcripts were targeted by miR-340 in HEK293 cells (Figure 5d).

These data reinforced the hypothesis that SKP2 could represent a target of miR-340, along with PUM1 and PUM2. To test the direct interaction with the putative miR-340 target sites in the *SKP2* transcript, we generated a luciferase construct containing the full-size *SKP2* 3′-UTR, along with four constructs containing site-directed mutations in each of the hexanucleotides complementary to the miR-340 seed (Figure 5e). Although the empty vector was unaffected, the luciferase-*SKP2*-3′-UTR construct exhibited an almost twofold repression in response to miR-340. The mutations hitting the three distal sites did not affect the miR-340-mediated repression, whereas the inhibition was almost completely relieved by mutating the seed of the upstream element (Figure 5e). Unlike the other sites, the upstream element exhibits high inter-species conservation (Supplementary Figure S3C). In agreement with the results of Figure 5, RT–PCR analysis showed that the *SKP2* isoforms 1 and 3, sharing the upstream miR-340 target element, were downregulated in response to

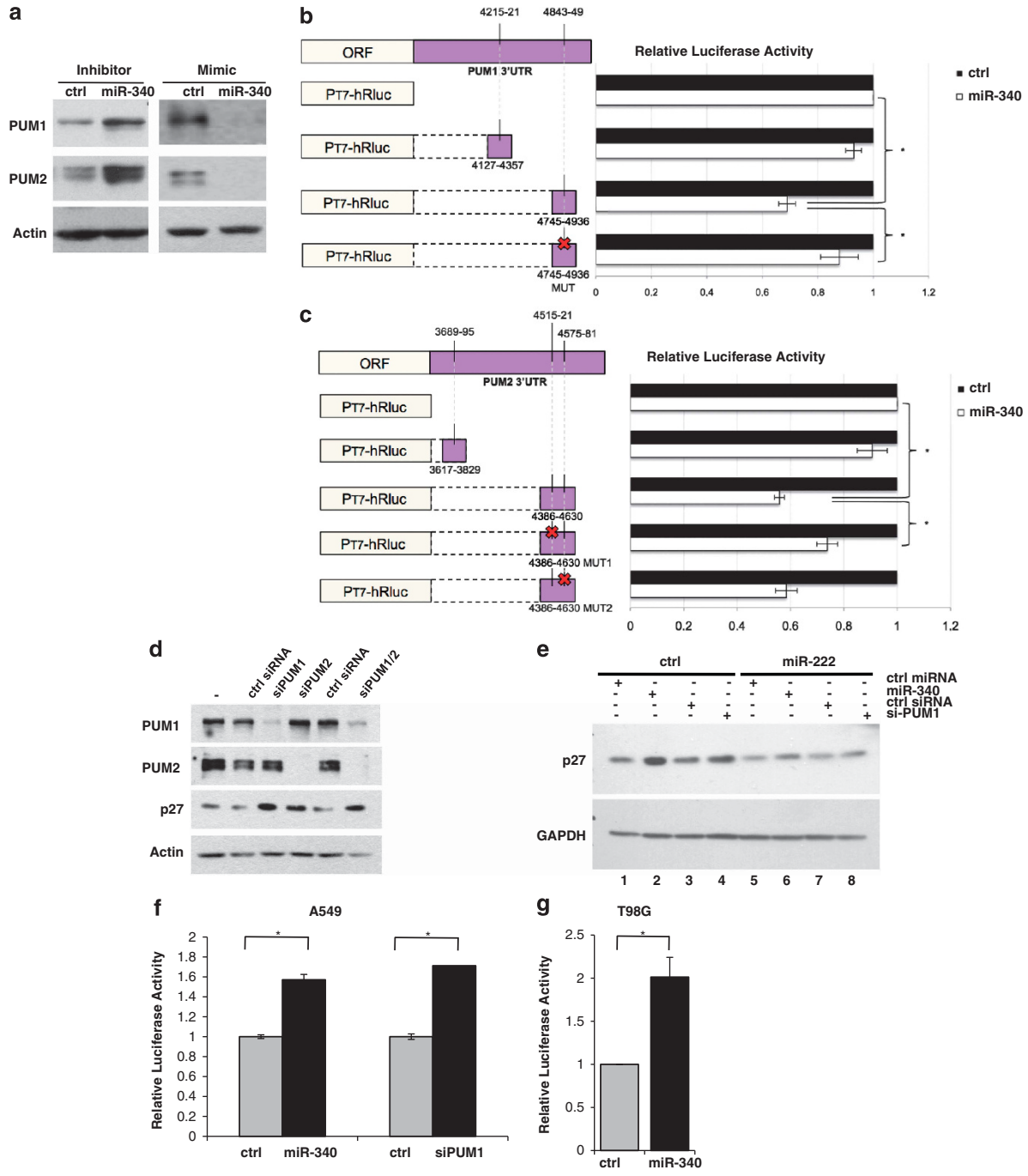

Figure 3. miR-340 targets the PUM1 and PUM2 transcripts, which are required for the miR-222-mediated downregulation of p27. (**a**) Western blotting analysis of PUM1 and PUM2 in A549 cells, 48 h after transfection with the LNA anti-miR-340 or miR-340 mimic vs LNA or mimic controls. The beta-actin signals, for control of equal loading, are the same as in Figures 2a and 5b, because the samples derive from the same blot. (**b**) Left: scheme of the *PUM1* 3′-UTR, showing the position of predicted miR-340 target sites with respect to the ATG of the CDS and the fragments cloned downstream of the luciferase reporter, including the site-directed mutation of the distal miR-340 seed. Right: normalized luciferase activity expressed by the luc-*PUM1* 3′-UTR constructs, cotransfected with the miR-340 mimic vs control in A549 cells. Error bars represent the mean ± s.d. of three independent experiments. Two-tail *t*-test results are indicated by $*P \leqslant 0.05$. (**c**) Left: scheme of the *PUM2* 3′-UTR, showing the position of predicted miR-340 target sites with respect to the ATG of the protein and the fragments cloned downstream of the luciferase reporter, including the site-directed mutation of the two distal miR-340 seeds. Right: normalized luciferase activity expressed by the luc-*PUM2* 3′-UTR constructs, cotransfected with the miR-340 mimic vs control in A549 cells. Error bars represent the mean ± s.d. of three independent experiments. Two-tail *t*-test results are indicated by $*P \leqslant 0.05$. (**d**) Western blotting analysis of p27 vs PUM1 and PUM2 protein levels in A549 cells transfected with siRNAs interfering with PUM1 and/or PUM2 expression after 48 h. Beta-actin serves as a loading control. (**e**) Western blotting analysis of p27 expression in A549 cells transfected for 72 h with the miR-340 mimic or the PUM1-specific siRNA, alone or in combination with the miR-222 mimic, compared with the indicated nontargeting controls. GAPDH serves as a loading control. (**f** and **g**) Relative luciferase activity expressed by the psiCHECK2 *p27*-3′-UTR construct, following cotransfection for 48 h with the miR-340 mimic vs control or anti-PUM1 vs control siRNA in A549 and the miR-340 mimic vs control in T98G cells. Error bars represent the mean ± s.d. of three independent experiments. Two-tail *t*-test results are indicated by $*P \leqslant 0.05$.

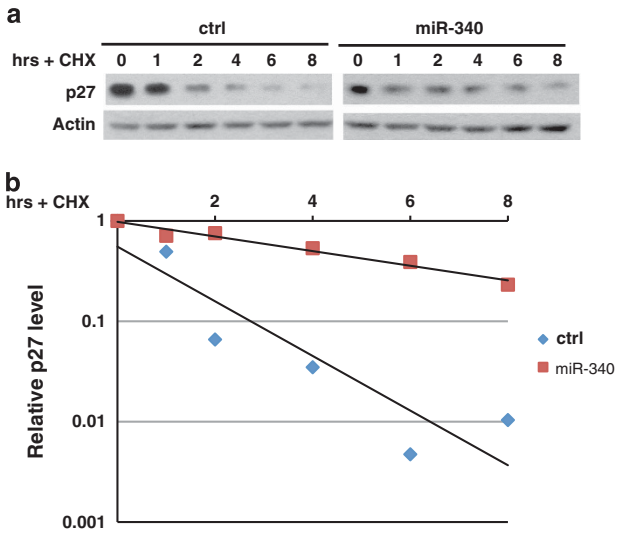

Figure 4. miR-340 increases the p27 protein stability. (**a**) Immunoblotting analysis of the p27 decay, analyzed by cycloheximide (CHX) chase assay. p27 levels are visualized in A549 cells transfected with the control or miR-340 mimic, after the addition of CHX (50 μg/ml) at the indicated time points. (**b**) Half-life of p27 in presence of miR-340 mimic vs control, determined by densitometric quantitation and normalization of the p27 signal by beta-actin in the western blot panel (**a**). The experiment was repeated three times with comparable kinetics.

miR-340 overexpression (Supplementary Figure S3D). Therefore, the *SKP2* transcript represents a *bona fide* target of miR-340, which represses SKP2 expression by interacting with a regulatory site shared by two out of the three SKP2 splice isoforms.

PUM1/2 and SKP2 downregulation mimics the effect of miR-340 on A549 cell viability and apoptosis

Having identified PUM1, PUM2 and SKP2 as miR-340 targets implicated in the negative control of p27 expression, we tested if the knockdown of the three regulators of p27 could mimic the effects of miR-340.

While knocking down PUM1 strongly inhibited the A549 growth rate and PUM2 inhibition only slightly affected cell viability (Figure 6a), SKP2 silencing exhibited an intermediate effect between PUM1 and PUM2 (Figure 6b).

These results were confirmed by clonogenic assays, which showed a stronger growth inhibition by the PUM1 vs SKP2 knockdown. Although the effect of the two individual siRNAs was smaller than the effect of miR-340, the double knockdown (PUM1 +SKP2) resulted in a cell growth inhibition even stronger than that induced by miR-340 (Figures 6c and d). Finally, we tested the effect of silencing PUM1 and/or SKP2 on A549 cell apoptosis. The fold increase of caspase 3/7 activity agreed with the results of cell viability and clonogenic assays, showing that the PUM1 knockdown was more proapoptotic than the SKP2 knockdown, whereas co-silencing both miR-340 targets caused the strongest increase of caspase activity (Figure 6e). Therefore, the combined inhibition of both PUM1 and SKP2 is able to recapitulate the effects of miR-340 on A549 cell viability and apoptosis. Finally, we tested if the p27 inhibition was able to antagonize the effect of miR-340 on A549 cell viability. The results showed that the miR-340-induced cell growth inhibition and apoptosis was only partially relieved by p27 knockdown (Supplementary Figure S4), thus suggesting additional roles of SKP2/PUM1-dependent p27-independent mechanisms downstream to miR-340.

miR-340 affects morphology, motility and multiple promigratory proteins in lung adenocarcinoma cells

According to our recent report,[22] miR-340-induced cell scattering and cytoskeletal rearrangements in A549 cells (Supplementary Figure S5A). Therefore, we decided to investigate if the miR-340-induced cell scattering was associated with changes in cell motility. Interestingly, transwell assays revealed that miR-340 overexpression significantly inhibited the migration of A549 cells (Supplementary Figure S5B).

Then, we investigated the expression of c-Met and Rock1, recently characterized as miR-340 targets implicated in the miR-340-mediated inhibition of cell motility and invasion in breast cancer[29] and osteosarcoma cells.[30] Both c-Met and Rock1 were downregulated in response to miR-340 overexpression (Supplementary Figure S5C).

Interestingly, the transcript encoding for the RhoA GTPase, representing the main activator of Rock1, harbors a conserved miR-340 site. We also observed that the *CDH1* mRNA, encoding for E-cadherin, contains a conserved miR-340 target site (Supplementary Figures S5D and E). Accordingly, the ectopically expressed miR-340 significantly inhibited both RhoA and E-Cadherin expression levels (Supplementary Figure S5C).

These results confirm c-Met and Rock1 as targets of miR-340 and suggest that the miR-340-mediated inhibition of RhoA and E-cadherin participates to the miR-340 effects on stress fibers, intercellular adhesion and cell migration.

miR-340 is downregulated in non-small cell lung adenocarcinoma

The above data, showing that miR-340 overexpression induces growth arrest and apoptosis along with decreased motility in A549 cells, suggested the possibility that miR-340 could be downregulated during lung cancer progression. Therefore, we analyzed miR-340 expression in a series of NSCLC tumor specimens. Clinical features of patients are summarized in Table 1 (Supplementary Information). Given the unavailability of matched healthy samples and the small size of individual subgroups representing the four stages of the disease, we compared the subset of T1/T2 vs T3/T4 patients. Analysis of 23 clinical samples showed that miR-340 expression was significantly lower ($P < 0.05$) in patients at more advanced compared with earlier stages of disease (Figure 7a). No correlation was observed with tumor histology, sex and age of patients. These results, along with the *in vitro* analysis, point to miR-340 as a novel tumor suppressor miRNA implicated in lung tumor progression.

DISCUSSION

We have previously identified miR-340 within a subset of miRNAs predicted to regulate the TGF-beta pathway. While miR-93, miR-519d and miR-190 were able to antagonize the TGF-beta-induced scattering of A549 cells, miR-340 induced cell scattering independently of TGF-beta.[22] These findings prompted us to investigate the impact of miR-340 on the neoplastic phenotype. Here, we have characterized the tumor suppressor activity of miR-340 in lung and glioblastoma cancer cells. The miR-340-mediated cell growth inhibition and apoptosis correlates with the accumulation of p27, resulting from the miR-340-mediated downregulation of three posttranscriptional regulators (PUM1, PUM2 and SKP2) of p27. While PUM1 and PUM2 inhibit p27 at the translational level, by rendering the p27 transcript available to interact with two oncomiRs (miR-221 and miR-222) overexpressed in lung and glioblastoma tumor cells, SKP2 inhibits the CDK inhibitor at the posttranslational level, by triggering the proteasomal degradation of p27 (summarized in Figure 8). The miR-340-mediated inhibition of cell motility correlates with the downregulation of two previously validated (c-Met and Rock1) and two candidate (RhoA and E-cadherin) miR-340 targets, implicated in cytoskeletal reorganization, cytokinesis and

intercellular adhesion. The analysis of NSCLC clinical specimens, showing the inverse correlation between miR-340 expression and lung cancer progression, points to miR-340 as a novel oncosuppressor in NSCLC.

miR-340 overexpression strongly inhibited whereas the miR-340 inhibitor stimulated proliferation, in both lung adenocarcinoma and glioblastoma cells (Figures 1 and 2), in agreement with similar observations in neuroblastoma, colorectal adenocarcinoma and

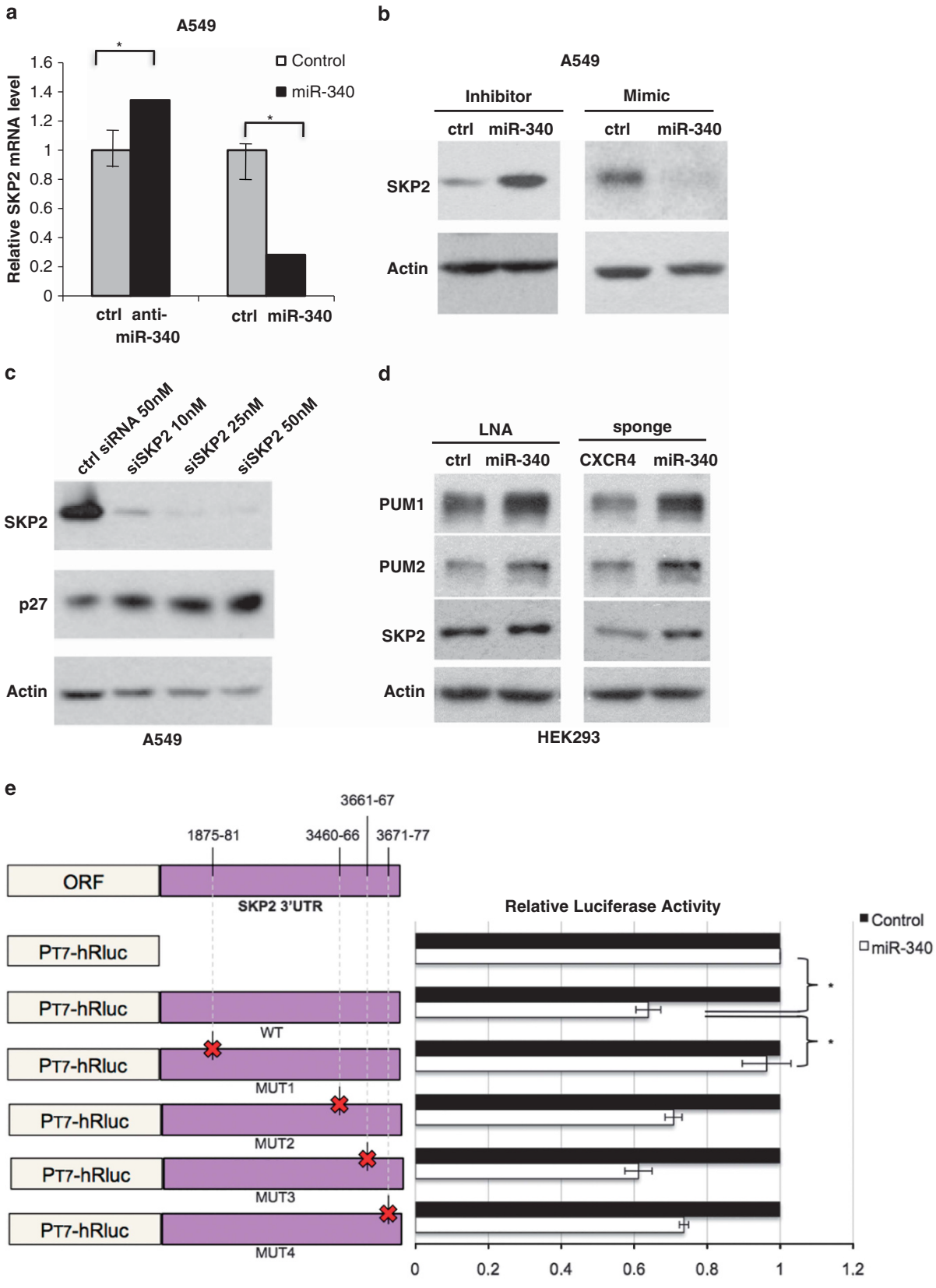

osteosarcoma.[30–32] The miR-340-mediated inhibition of cell viability was associated with both inhibition of DNA replication and increased basal apoptosis (Figure 1).

Although previous reports did not address the mechanisms implicated in the miR-340-mediated cell growth inhibition, our analyses suggest that the increased expression of p27 is a determinant of the miR-340-induced growth arrest. The decreased cell viability associated with increased apoptosis, in response to miR-340 overexpression, (Figures 2 and 6) is partially consequent to the miR-340-induced accumulation of p27. Accordingly, it has been shown that stable overexpression of p27 induces apoptotic death in A549 cells.[33]

During tumorigenesis, p27 is inactivated through multiple mechanisms, including impaired synthesis, increased protein degradation and mislocalization.[17] The here-described miR-340-mediated inhibition of multiple negative regulators of p27 puts an additional layer of complexity on the control mechanisms of the *CDKN1B* gene product. By rendering the *p27* 3′-UTR accessible to miR-221/222, both human *Pumilio* family members are required for the growth-induced downregulation of p27. In response to growth factor stimulation, PUM1 phosphorylation and accumulation results in the increased binding to the *p27* 3′-UTR and consequent downregulation of p27 during cell cycle progression.[16] We postulate that the loss of miR-340 results in the increased expression of both PUM1 and PUM2, which are required for the downregulation of p27 in tumors overexpressing miR-221/222 (Figure 8). Our results (Figure 3 and Supplementary Figure S2) indicate that PUM1 and PUM2 play interchangeable functions in p27 posttranscriptional regulation. Remarkably, the two transcripts, although lacking any significant homology in their 3′-UTRs, retain miR-340 target elements. Given the general role of *Pumilio* proteins as posttranscriptional regulators of gene expression,[34] in addition to p27, other transcripts controlling cell cycle progression might be affected by miR-340 through PUM1/PUM2-mediated mechanisms. Our data (Figure 6), showing that PUM1 inhibition affects the A549 cell proliferation more than PUM2, suggest that PUM1 might be involved in the posttranscriptional control of other cell cycle inhibitors besides p27.

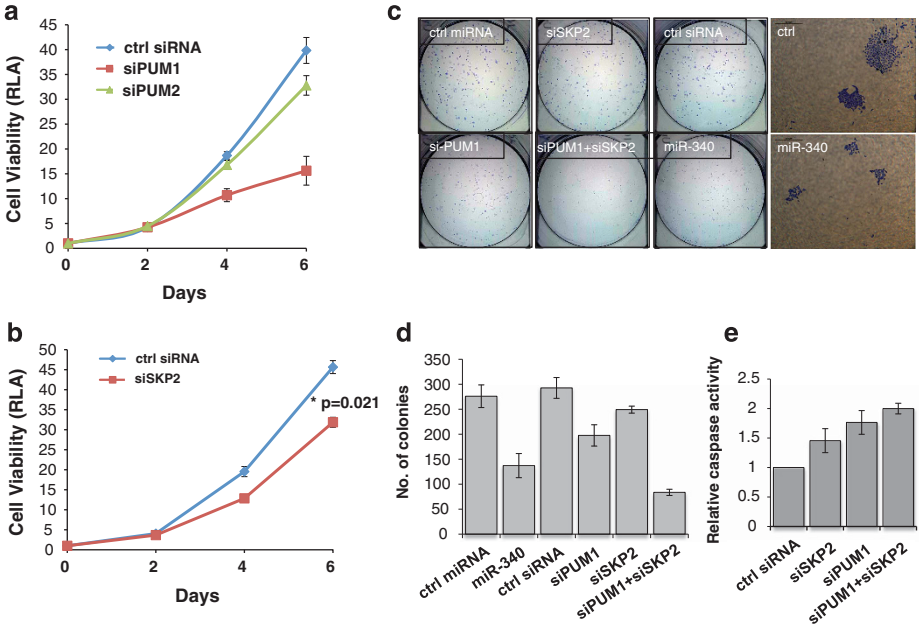

Figure 6. The knockdown of SKP2 or PUM1 partially recapitulates the effect of miR-340 on A549 cell proliferation and apoptosis. Growth rate of A549 cells transfected with the PUM1 or PUM2 (**a**) or SKP2 (**b**) specific siRNAs vs control siRNAs. Viable cells were determined by luminometric assays at the indicated time points. (**c**) Clonogenic assays. A549 cells, transfected with the PUM1 and/or SKP2 siRNA or the miR-340 mimic vs controls, were seeded in six-well dishes (500 cells per dish). Crystal violet-stained colonies were photographed after one week. Right panel shows a magnified image of miR-340 mimic vs control transfected cells. (**d**) Mean number of colonies. Error bars represent the mean ± s.d. of three independent experiments. (**e**) Caspase 3/7 activity in A549 cells 96 h following transfection with the PUM1 and/or SKP2 siRNAs vs siRNA control. Error bars represent the mean ± s.d. of three independent experiments.

Figure 5. The SKP2 transcript is a direct target of miR-340 (**a**) qRT–PCR and (**b**) western blotting analysis of *SKP2* mRNA and protein levels in A549 cells transfected with LNA-anti-miR-340 or miR-340 mimic vs LNA or mimic controls for 24 h for qRT–PCR or 48 h for western blotting, with GAPDH serving as an internal control in the qRT–PCR and beta-actin as a loading control in the western blot. The beta-actin signals are the same as in Figures 2a and 3a, because the samples derive from the same blot. Error bars represent the mean ± s.d. of three independent experiments. Two-tail *t*-test results are indicated by $*P \leqslant 0.05$. (**c**) Western blot analysis of the effect of SKP2 knockdown on p27 expression, 48 h after transfection with the SKP2-specific siRNA (10nM, 25nM and 50nM) in A549 cells vs siRNA control. Beta-actin serves as a loading control. Following densitometric analysis and normalization vs the beta-actin signal, SKP2 was decreased by 7.7-fold, 33-fold and 29-fold in response to the increasing amount of the siRNA. (**d**) Western blotting analysis of PUM1, PUM2 and SKP2 in HEK293 cells. Left: cells were transfected with LNA-anti-miR-340 vs control for 48 h. Right: cells were transfected with miR-340 sponge expression vector vs empty vector (CXCR4) for 48 h. Beta-actin serves as a loading control. (**e**) Diagram of the 2388-nt *SKP2* 3′-UTR, showing the position of predicted miR-340 target sites with respect to the ATG of the protein and the fragment cloned downstream of the luciferase reporter, with the mutations disrupting the four miR-340 seeds. Right: normalized luciferase activity expressed by the indicated psiCHECK2 *SKP2* 3′-UTR constructs, cotransfected with the miR-340 mimic vs control in A549 cells. Error bars represent the mean ± s.d. of three independent experiments. Two-tail *t*-test results are indicated by $*P \leqslant 0.05$.

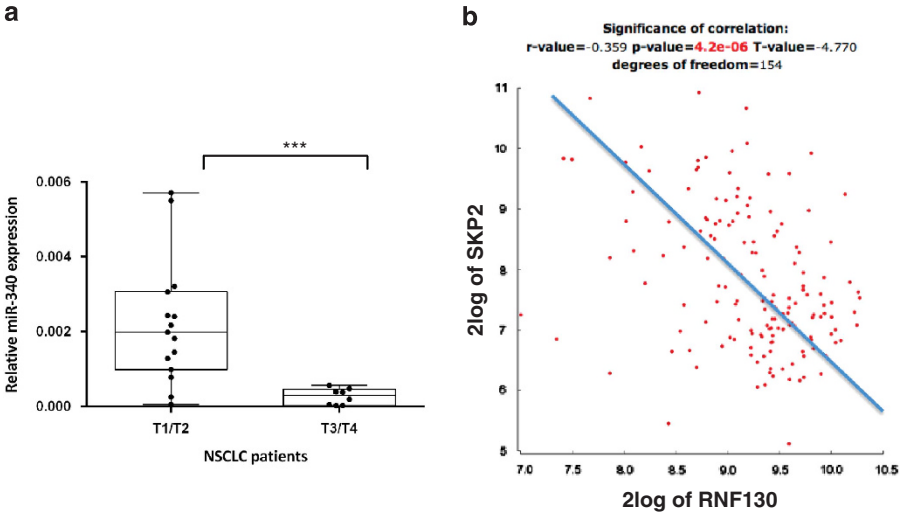

Figure 7. Reduced expression of miR-340 in human lung cancer tissue specimens. (**a**) miR-340 expression was analyzed by qRT–PCR, using U6 as an internal control, in RNA samples extracted from surgical tissue specimens of 23 NSCLC-affected patients at different tumor node metastasis (TNM) staging (T1-T2-T3-T4), as indicated. Box-plot diagram of miR-340 expression in the T1/T2 and T3/T4 groups. The horizontal lines indicate the median while the whiskers represent the minimum and maximum values for each group. The asterisks indicated a *P*-value < 0.05. (**b**) Analysis of *SKP2* vs *RNF130* expression in a cohort of 91 NSCLC patients.[38] The diagram shows the inverse correlation between *SKP2* vs *RNF130* expression levels. Dataset analysis was performed by using the R2 microarray analysis and visualization platform (http://r2.amc.nl).

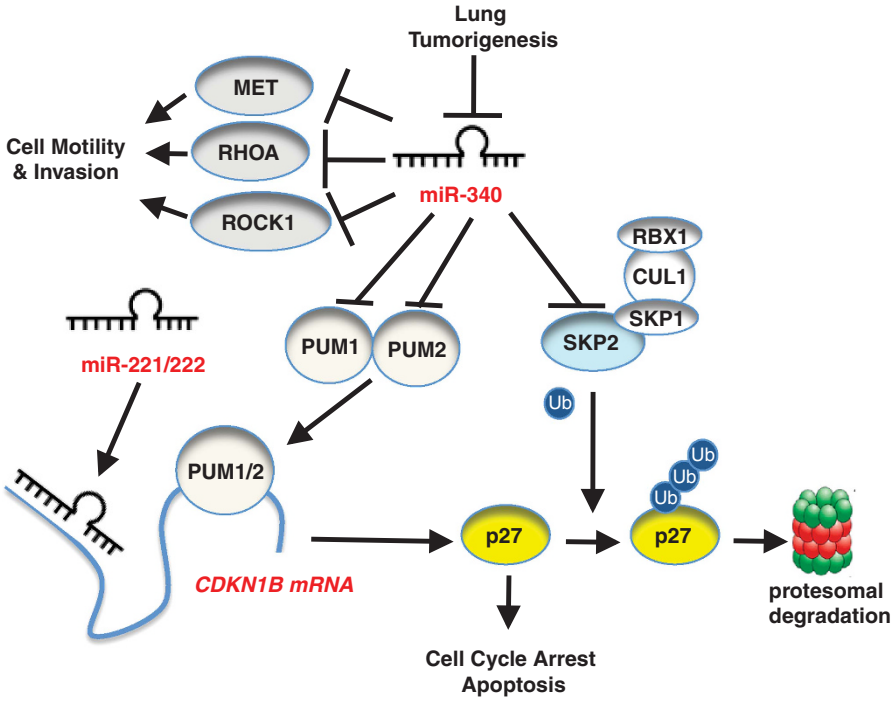

Figure 8. The model summarizes the here described roles of miR-340 in lung tumor cells. In addition to inhibiting multiple regulators of cell motility (MET, RHOA, ROCK1), miR-340 induces the accumulation of p27 and cell cycle arrest by targeting three negative regulators of p27: PUM1, PUM2 and SKP2. The drawing represents how the binding of PUM1 or PUM2 induces an RNA structure that renders the *p27* 3′-UTR accessible to miR-221/222-mediated translational repression,[16] while SKP2, along with the other components of the SCF complex, induces the polyubiquitylation and proteasomal degradation of p27.

Alternatively, PUM2, in addition to inhibiting p27 expression, might control other positive regulator(s) of the cell cycle. Remarkably, the transcriptome-wide analysis of the mRNAs interacting with PUM1 and PUM2 in human cancer cells shows that the sets of PUM1- and PUM2- associated transcripts are strongly overlapping, but not identical. Moreover, the strong enrichment of the *Pumilio* binding sites around predicted miRNA target sequences in the 3′-UTRs of experimentally determined PUM1 and PUM2 targets suggests that miR-340 might affect other miRNA–mRNA interactions, in addition to the binding of miR-221-/222 to the *p27* coding transcript.[34] Another key regulator of cell proliferation, E2F3, is cooperatively regulated by *Pumilio* proteins and miRNAs, thus suggesting that miR-340 could indirectly control E2F3 along with the p27 expression.[35] In addition, PUM2 can also

play miRNA-independent roles, by stabilizing and activating Aurora-A kinase in the induction of mitotic entry.[36] Therefore, the impact of miR-340 on cell cycle progression might result from the balance between the antagonistic effects of PUM1 and PUM2 downregulation on p27, E2F3 and Aurora-A kinase expression.

miR-340 affected not only the synthesis but also the decay of p27, by a mechanism dependent on the miR-340-mediated downregulation of the SKP2 ubiquitin ligase (Figures 4 and 5), which represents the rate-limiting component of the SCF^{SKP2} complex. Our results show, for the first time, that the expression of the human SKP2 oncoprotein is subjected to miRNA-mediated posttranscriptional regulation. Given the oncosuppressor roles played by miR-340 in other solid tumors,[29–32] the possible miR-340-mediated control of SKP2 deserves further investigations in other tumors, such as neuroblastoma, colorectal adenocarcinoma and osteosarcoma.

In addition to inducing growth arrest and apoptosis, miR-340 caused cell scattering and cytoskeletal rearrangements[22] (Supplementary Figure S5), along with inhibition of motility in A549 cells. These data are in line with the recent identification of transcripts encoding several proinvasive proteins, as targets of miR-340. The oncoprotein c-Met, implicated in the miR-340-mediated inhibition of breast cancer cell migration,[29] was only slightly affected by miR-340, thus suggesting that other miR-340 targets, such as RhoA and Rock1, strongly downregulated in response to the ectopic miRNA (Supplementary Figure S5), could mediate the miR-340 effect on A549 cell motility. Accordingly, Rock1 has been recently validated as a miR-340 target, implicated in the control of migration and invasion in osteosarcoma cells.[30] In addition, our data (Supplementary Figure S5), suggest that the direct inhibition of E-cadherin mRNA is probably involved in the miR-340-induced loss of intercellular adhesion.

Several recent reports indicate that miR-340 is downregulated in multiple tumors.[29–32] The cancer-associated downregulation of miR-340 emerged from the miRNA expression profiling of the NCI-60 human cancer cell lines. miR-340 was included among candidate oncosuppressor miRNAs, because of its downregulation in CNS-derived tumor cell lines.[23] Accordingly, in neuroblastoma, miR-340 has been identified in a subset of epigenetically silenced miRNAs, which could be reactivated by ATRA-induced demethylation of CpG-rich regions associated with putative miRNA transcriptional regulatory elements.[31] Similarly, miR-340 downregulation in gastric cancer has been found associated with methylation of a CpG island in the promoter region of the miR-340 host gene.[37] ENCODE-based analysis of the major histone marks associated with transcriptional promoters (H3K4Me3), suggests the absence of internal promoters within the introns of the miR-340 host gene (*RNF130*) (Supplementary Figure S6), thus indicating that miR-340 is co-transcribed with its host gene. Accordingly, miR-340 and *RNF130* were concordantly expressed in NSCLC cell lines (Supplementary Figure S7). Therefore, we utilized *RNF130* as a proxy for miR-340 expression in publicly available databases of microarray-based analyses of lung tumors. The inverse correlation between *RNF130* and *SKP2* expression (Figure 7b and Supplementary Figure S8) in a series of 156 samples, representing a cohort of 91 NSCLC patients[38] suggests that miR-340 is actually involved in the *in vivo* regulation of SKP2 in NSCLC patients. Because SKP2 overexpression represents a poor prognostic marker in NSCLC,[39] it will be interesting to investigate the predictive value of prognostic correlations based on miR-340 vs SKP2 expression in lung tumor samples. Interestingly, the combined profiling of miR-340 and *ROCK1* mRNA has been recently shown to predict tumor progression and prognosis in pediatric osteosarcoma, in which patients exhibiting miR-340-low/*ROCK1*-high expression levels show the worst outcome.[40]

Accordingly, miR-340 expression inversely correlates with disease progression in breast cancer, in which the lowest miR-340 levels correlate with lymphonodal metastasis.[29] miR-340 displays positive prognostic correlations also in stage III colorectal cancer, being upregulated in patients with better survival, compared with patients exhibiting lower 5-year survival rates.[32]

Altogether, these findings indicate that miR-340 is a novel prognostic marker in multiple tumor types. Given the strong miR-340-mediated tumor suppression evidenced by our analysis, along with the highly promising therapeutic approaches based on re-expression of tumor suppressor miRNAs,[21] further studies are warranted, to explore the potential of miR-340 as a therapeutic tool in NSCLC.

MATERIALS AND METHODS

Cell lines (ATCC, Rockville, MD, USA) were cultured in DMEM (Gibco, Invitrogen, Carlsbad, CA, USA), supplemented with 10% fetal bovine serum (Gibco, Invitrogen) and penicillin (100 U/ml) streptomycin (100 U/ml) (Lonza, Basel, Switzerland). miRNA and LNA transfections, luciferase reporter assays, immunoblotting, cycloheximide chase analysis and qRT-–PCR were carried out as described previously.[41,42] Cell cycle distribution was analyzed by the Becton Dickinson FACSCanto A (Becton, Dickinson and Company, Franklin Lakes, NJ, USA). Cell migration was analyzed by Transwell® Permeable Supports (Costar, Corning Inc., Corning, NY, USA). Cell viability and caspase activity were detected by CellTiter-Glo® and Caspase-3/7-Glo® (Promega, Madison, WI, USA). Immunofluorescence images were visualized using a Zeiss LSM710 confocal microscope (Zeiss, Oberkochen, Germany).

CONFLICT OF INTEREST

The authors declare no conflict of interest.

ACKNOWLEDGEMENTS

We thank Reuven Agami, Judy Lieberman and Vladimir Spiegelman for expression vectors. We also thank the IGB FACS and Microscopy facilities. This work was supported by the AIRC (Associazione Italiana per la Ricerca sul Cancro) Grant-10489, AICR (Association for International Cancer Research, UK) Grant-08-182 and MERIT Grant-RBNE08YFN3 (MIUR) to Pasquale Verde. Gerolama Condorelli was supported by grants from AIRC (Grant-14046) and Fondazione Berlucchi.

REFERENCES

1 Esquela-Kerscher A, Slack FJ. Oncomirs—microRNAs with a role in cancer. *Nat Rev Cancer* 2006; **6**: 259–269.
2 Croce CM. Causes and consequences of microRNA dysregulation in cancer. *Nat Rev Genet* 2009; **10**: 704–714.
3 Jansson MD, Lund AH. MicroRNA and cancer. *Mol Oncol* 2012; **6**: 590–610.
4 van Kouwenhove M, Kedde M, Agami R. MicroRNA regulation by RNA-binding proteins and its implications for cancer. *Nat Rev Cancer* 2011; **11**: 644–656.
5 Aqeilan RI, Calin GA, Croce CM. miR-15a and miR-16-1 in cancer: discovery, function and future perspectives. *Cell Death Differ* 2009; **17**: 215–220.
6 Bandi N, Zbinden S, Gugger M, Arnold M, Kocher V, Hasan L *et al.* miR-15a and miR-16 are implicated in cell cycle regulation in a Rb-dependent manner and are frequently deleted or down-regulated in non-small cell lung cancer. *Cancer Res* 2009; **69**: 5553–5559.
7 Hermeking H. The miR-34 family in cancer and apoptosis. *Cell Death Differ* 2010; **17**: 193–199.
8 Petrocca F. E2F1-regulated microRNAs impair TGFβ-dependent cell-cycle arrest and apoptosis in gastric cancer. *Cancer Cell* 2008; **13**: 272–286.
9 le Sage C, Nagel R, Egan DA, Schrier M, Mesman E, Mangiola A *et al.* Regulation of the p27(Kip1) tumor suppressor by miR-221 and miR-222 promotes cancer cell proliferation. *EMBO J* 2007; **26**: 3699–3708.
10 Medina R, Zaidi SK, Liu C-G, Stein JL, vanWijnen AJ, Croce CM *et al.* MicroRNAs 221 and 222 bypass quiescence and compromise cell survival. *Cancer Res* 2008; **68**: 2773–2780.
11 Galardi S, Mercatelli N, Giorda E, Massalini S, Frajese GV, Ciafre SA *et al.* miR-221 and miR-222 expression affects the proliferation potential of human prostate carcinoma cell lines by targeting p27Kip1. *J Biol Chem* 2007; **282**: 23716–23724.
12 Visone R, Russo L, Pallante P, De Martino I, Ferraro A, Leone V *et al.* MicroRNAs (miR)-221 and miR-222, both overexpressed in human thyroid papillary carcinomas, regulate p27Kip1 protein levels and cell cycle. *Endocr Relat Cancer* 2007; **14**: 791–798.

13 Fornari F, Gramantieri L, Ferracin M, Veronese A, Sabbioni S, Calin GA *et al.* MiR-221 controls CDKN1C/p57 and CDKN1B/p27 expression in human hepatocellular carcinoma. *Oncogene* 2008; **27**: 5651–5661.
14 Nassirpour R, Mehta PP, Baxi SM, Yin M-J. miR-221 promotes tumorigenesis in human Triple negative breast cancer cells. *PLoS ONE* 2013; **8**: e62170.
15 Garofalo M, Leva GD, Romano G, Nuovo G, Suh S-S, Ngankeu A *et al.* miR-221&222 regulate TRAIL resistance and enhance tumorigenicity through PTEN and TIMP3 downregulation. *Cancer Cell* 2009; **16**: 498–509.
16 Kedde M, van Kouwenhove M, Zwart W, Oude Vrielink JAF, Elkon R, Agami R. A Pumilio-induced RNA structure switch in p27-3′ UTR controls miR-221 and miR-222 accessibility. *Nat Cell Biol* 2010; **12**: 1014–1020.
17 Chu IM, Hengst L, Slingerland JM. The Cdk inhibitor p27 in human cancer: prognostic potential and relevance to anticancer therapy. *Nat Rev Cancer* 2008; **8**: 253–267.
18 Frescas D, Pagano M. Deregulated proteolysis by the F-box proteins SKP2 and beta-TrCP: tipping the scales of cancer. *Nat Rev Cancer* 2008; **8**: 438–449.
19 Nakayama K, Nagahama H, Minamishima YA, Miyake S, Ishida N, Hatakeyama S *et al.* Skp2-mediated degradation of p27 regulates progression into mitosis. *Dev Cell* 2004; **6**: 661–672.
20 Lin P-Y, Yu S-L, Yang P-C. MicroRNA in lung cancer. *Br J Cancer* 2010; **103**: 1144–1148.
21 Kasinski AL, Slack FJ. Epigenetics and genetics. MicroRNAs en route to the clinic: progress in validating and targeting microRNAs for cancer therapy. *Nat Rev Cancer* 2011; **11**: 849–864.
22 Gennarino VA, D'Angelo G, Dharmalingam G, Fernandez S, Russolillo G, Sanges R *et al.* Identification of microRNA-regulated gene networks by expression analysis of target genes. *Genome Res* 2012; **22**: 1163–1172.
23 Gaur A, Jewell DA, Liang Y, Ridzon D, Moore JH, Chen C *et al.* Characterization of microRNA expression levels and their biological correlates in human cancer cell lines. *Cancer Res* 2007; **67**: 2456–2468.
24 Dong H, Luo L, Hong S, Siu H, Xiao Y, Jin L *et al.* Integrated analysis of mutations, miRNA and mRNA expression in glioblastoma. *BMC Syst Biol* 2010; **4**: 163.
25 le Sage C, Nagel R, Agami R. Diverse ways to control p27Kip1 function: miRNAs come into play. *Cell Cycle* 2007; **6**: 2742–2749.
26 Zhang C. PUMA is a novel target of miR-221/222 in human epithelial cancers. *Int J Oncol* 2010; **37**: 1–6.
27 Rehmsmeier M, Steffen P, Hochsmann M, Giegerich R. Fast and effective prediction of microRNA/target duplexes. *RNA* 2004; **10**: 1507–1517.
28 Goswami S, Tarapore RS, Teslaa JJ, Grinblat Y, Setaluri V, Spiegelman VS. MicroRNA-340-mediated degradation of microphthalmia-associated transcription factor mRNA is inhibited by the coding region determinant-binding protein. *J Biol Chem* 2010; **285**: 20532–20540.
29 Wu Z-S, Wu Q, Wang C-Q, Wang X-N, Huang J, Zhao J-J *et al.* miR-340 inhibition of breast cancer cell migration and invasion through targeting of oncoprotein c-Met. *Cancer* 2011; **117**: 2842–2852.
30 Zhou X, Wei M, Wang W. MicroRNA-340 suppresses osteosarcoma tumor growth and metastasis by directly targeting ROCK1. *Biochem Biophys Res Commun* 2013; **437**: 653–658.
31 Das S, Bryan K, Buckley PG, Piskareva O, Bray IM, Foley N *et al.* Modulation of neuroblastoma disease pathogenesis by an extensive network of epigenetically regulated microRNAs. *Oncogene* 2012; **32**: 2927–2936.
32 Hu Y. miR-124, miR-137 and miR-340 regulate colorectal cancer growth via inhibition of the Warburg effect. *Oncol Rep* 2012; **28**: 1346–1352.
33 Wang X, Gorospe M, Huang Y, Holbrook NJ. p27Kip1 overexpression causes apoptotic death of mammalian cells. *Oncogene* 1997; **15**: 2991–2997.
34 Galgano A, Forrer M, Jaskiewicz L, Kanitz A, Zavolan M, Gerber AP. Comparative analysis of mRNA targets for human PUF-family proteins suggests extensive interaction with the miRNA regulatory system. *PLoS ONE* 2008; **3**: e3164.
35 Miles WO, Tschöp K, Herr A, Ji J-Y, Dyson NJ. Pumilio facilitates miRNA regulation of the E2F3 oncogene. *Genes Dev* 2012; **26**: 356–368.
36 Huang Y-H, Wu C-C, Chou C-K, Huang C-YF. A translational regulator, PUM2, promotes both protein stability and kinase activity of Aurora-A. *PLoS ONE* 2011; **6**: e19718.
37 Hashimoto Y, Akiyama Y, Yuasa Y. Multiple-to-multiple relationships between microRNAs and target genes in gastric cancer. *PLoS ONE* 2013; **8**: e62589.
38 Hou J, Aerts J, Hamer den B, van IJcken W, Bakker den M, Riegman P *et al.* Gene expression-based classification of non-small cell lung carcinomas and survival prediction. *PLoS ONE* 2010; **5**: e10312.
39 Takanami I. The prognostic value of overexpression of Skp2 mRNA in non-small cell lung cancer. *Oncol Rep* 2005; **13**: 727–731.
40 Cai H, Lin L, Cai H, Tang M, Wang Z. Combined microRNA-340 and ROCK1 mRNA profiling predicts tumor progression and prognosis in pediatric osteosarcoma. *IJMS* 2014; **15**: 560–573.
41 Talotta F, Cimmino A, Matarazzo MR, Casalino L, De Vita G, D'Esposito M *et al.* An autoregulatory loop mediated by miR-21 and PDCD4 controls the AP-1 activity in RAS transformation. *Oncogene* 2009; **28**: 73–84.
42 Talotta F, Mega T, Bossis G, Casalino L, Basbous J, Jariel-Encontre I *et al.* Heterodimerization with Fra-1 cooperates with the ERK pathway to stabilize c-Jun in response to the RAS oncoprotein. *Oncogene* 2010; **29**: 4732–4740.

Supplementary Information accompanies this paper on the Oncogene website (http://www.nature.com/onc)